arXiv:1010.4139v2 [hep-ph] 12 Mar 2012

The neutral heavy scalar productions associated with Z_L in the littlest Higgs model at ILC and CLIC

A. ÇAĞ̃IL* and M. T. ZEYREK†

Physics Department, Middle East Technical University,
06531 Ankara, Turkey
*ayse.cagil@cern.ch
†zeyrek@metu.edu.tr

In this work, the production processes of heavy neutral scalar and pseudo scalar associated with standard model gauge boson Z_L at future e^+e^- colliders (ILC and CLIC) are examined. The total and differential cross sections are calculated for the processes in the context of the littlest Higgs model. Also dependence of production processes to littlest Higgs model parameters in the range of compatibility with electroweak precision measurements and decays to lepton flavor violating final states are analyzed. We have found that both heavy scalar and pseudoscalar will be produced in e^+e^- colliders. Also the depending on the model parameters, the neutral heavy scalar can be reconstructed or lepton flavor violating signals can be observed.

Keywords: littlest Higgs model, heavy scalars, electron colliders, heavy Higgs, lepton flavor violation.

PACS numbers: 12.60.-i,13.66.Fg,13.66.Hk,14.80.Cp.

1. Introduction

Standard model (SM) is an effective theory with a cut off scale around electroweak symmetry breaking (EWSB) scale. However in SM, Higgs scalar, giving mass to fermions and gauge bosons gets loop corrections to its mass up to cut off scale, which is called the hierarchy problem. The little Higgs models[1, 2, 3, 4] are introduced to solve the hierarchy problem among the alternative solutions such as supersymmetry, extra dimensions and dynamical symmetry breaking models. The little Higgs models propose a solution by enlarging the symmetry group of the SM. The constraints on little Higgs models are studied[5, 6, 7, 8, 9, 10, 11], and the phenomenology of the little Higgs models are reviewed[12, 13, 14]. The little Higgs models are also expected to give significant signatures in future high energy colliders and studied [15, 16, 17, 18, 19, 20].

In the littlest Higgs model[1] as a result of enlarged symmetry group, there appears new vector gauge bosons and also a new heavy scalar triplet. The appearance of new scalars in the littlest Higgs model result in lepton flavor violation when a $5D$ operator is implemented in the Yukawa lagrangian[21, 22, 23, 24].

In this work we examined the production of neutral scalar (ϕ^0) and pseudo scalar (ϕ^P) associated with Z_L boson in the littlest Higgs model at e^+e^- colliders, namely, International Linear Collider (ILC) [25] and Compact Linear Collider (CLIC) [26]. To analyze the production rates, firstly the most promising channel $e^+e^- \to Z_L\phi^0$ is analyzed. Since the final signals of ϕ^0 and ϕ^P is same, to analyze the behavior of the final states for the energies ($\sqrt{s} > 1TeV$), the higher order production processes; $e^+e^- \to Z_L\phi^0\phi^0$, $e^+e^- \to Z_L\phi^P\phi^P$ and $e^+e^- \to Z_L\phi^0\phi^P$ are also examined. Since the process $e^+e^- \to Z_L\phi^P$ is not allowed in the littlest Higgs model, the latter two processes involving ϕ^P are also important for the ϕ^P production. Finally, lepton flavor violating signals of neutral scalars as *"Z_L+missing energy"* which characterizes the new neutral scalar and pseudoscalar to be littlest Higgs are analyzed[21].

In this paper, we present the relevant formulas and calculations in section 2. In section 3, the results and discussions are presented.

2. Theoretical Framework

In the littlest Higgs model global symmetry $SU(5)$ is broken spontaneously to $SO(5)$ at an energy scale $f \sim 1TeV$ leaving 14 Nambu Goldstone bosons(NGB) corresponding to broken symmetries. In the model $SU(5)$ contains the gauged subgroup $[SU(2)_1 \otimes U(1)_1] \otimes [SU(2)_2 \otimes U(1)_2]$. As a consequence symmetry breaking, gauge bosons gain mass by eating the four of the NGBs. The mixing angles between the $SU(2)$ subgroups and between the $U(1)$ subgroups are defined respectively as:

$$s \equiv \sin\theta = \frac{g_2}{\sqrt{g_1^2 + g_2^2}} \quad , \qquad s' \equiv \sin\theta' = \frac{g_2'}{\sqrt{g_1'^2 + g_2'^2}} \quad , \tag{1}$$

where g_i and g_i' are the gauge couplings of $SU(2)_i$ and $U(1)_i$ subgroups respectively. By EWSB vector bosons get extra mixings due to vacuum expectation values of h doublet and ϕ triplet resulting the final masses to the order of $\frac{v^2}{f^2}$ such as[13]:

$$\begin{aligned}
M^2_{A_L} &= 0, \\
M^2_{Z_L} &= m_z^2\left[1-\frac{v^2}{f^2}\left(\frac{1}{6}+\frac{1}{4}(c^2-s^2)^2+\frac{5}{4}(c'^2-s'^2)^2\right)+8\frac{v'^2}{v^2}\right], \\
M^2_{A_H} &= \frac{f^2g'^2}{20s'^2c'^2}-\frac{1}{4}g'^2v^2+g^2v^2\frac{x_H}{4s^2c^2} \qquad (2)\\
&= m_z^2s_{\rm w}^2\left(\frac{f^2}{5s'^2c'^2v^2}-1+\frac{x_Hc_{\rm w}^2}{4s^2c^2s_{\rm w}^2}\right), \\
M^2_{Z_H} &= \frac{f^2g^2}{4s^2c^2}-\frac{1}{4}g^2v^2-g'^2v^2\frac{x_H}{4s'^2c'^2} \qquad (3)\\
&= m_w^2\left(\frac{f^2}{s^2c^2v^2}-1-\frac{x_Hs_{\rm w}^2}{s'^2c'^2c_{\rm w}^2}\right),
\end{aligned}$$

where $m_z \equiv gv/(2c_{\rm w})$ and $x_H = \frac{5}{2}gg'\frac{scs'c'(c^2s'^2+s^2c'^2)}{(5g^2s'^2c'^2-g'^2s^2c^2)}$ and $s_{\rm w}$ and $c_{\rm w}$ are the usual weak mixing angles. The parameters v and v' are the vacuum expectation values of scalar doublet and triplet given as[13];

$$\langle h^0\rangle = v/\sqrt{2} \quad , \quad \langle i\phi^0\rangle = v' \leq \frac{v^2}{4f}, \qquad (4)$$

bounded by electroweak precision data, where $v = 246GeV$. Also diagonalizing the mass matrix for scalars the physical states are found to be the SM Higgs scalar H, the neutral scalar ϕ^0, the neutral pseudo scalar ϕ^P, and the charged scalars ϕ^+ and ϕ^{++}. The masses of the heavy scalars are degenerate, and in terms of Higgs mass expressed as[13]:

$$M_\phi = \frac{\sqrt{2}f}{v\sqrt{1-(\frac{4v'f}{v^2})^2}}M_H. \qquad (5)$$

The scalar fermion interactions in the model are written in Yukawa lagrangian preserving gauge symmetries of the model for SM leptons and quarks, including the third generation having an extra singlet, the T quark. The fermions in the littlest Higgs model can be charged under both $U(1)_1$ and $U(1)_2$ subgroups[10, 13]. Also for light fermions, a lepton number violating coupling can be implemented in Yukawa lagrangian[21, 22] which results in lepton flavor violation by unit two, such as:

$$\mathcal{L}_{LFV} = iY_{ij}L_i^T\ \phi C^{-1}L_j + \text{h.c.}, \qquad (6)$$

where L_i are the lepton doublets $\begin{pmatrix} l & \nu_l \end{pmatrix}$, and Y_{ij} are the elements of the mixing matrix with $Y_{ii} = Y$ and $Y_{ij(i \neq j)} = Y'$. The values of Yukawa couplings Y and Y' are restricted by the current constraints on the neutrino masses[27], given as; $M_{ij} = Y_{ij} v' \simeq 10^{-10} GeV$[21]. Since the vacuum expectation value v' has only an upper bound(Eq. 4), Y_{ij} can be taken up to order of unity without making v' unnaturally small.

The parameters f; the symmetry breaking scale , and s, s'; the mixing angles of the littlest Higgs model are not restricted by the model. These parameters are constrained by observables of electroweak precision data and the direct search for a heavy gauge bosons at Tevatron[5, 6, 7, 8, 9, 10]. In the case when fermions are charged under both $U(1)$ groups, the allowed parameter space is listed as follows. For the values of the symmetry breaking scale $1TeV \leq f \leq 2TeV$, mixing angles are in the range $0.75 \leq s \leq 0.99$ and $0.6 \leq s' \leq 0.75$, for $2TeV \leq f \leq 3TeV$ they have acceptable values in the range $0.6 \leq s \leq 0.99$ and $0.6 \leq s' \leq 0.8$, for $3TeV \leq f \leq 4TeV$ they are in the range $0.4 \leq s \leq 0.99$ and $0.6 \leq s' \leq 0.85$, and for the higher values of the symmetry breaking scale, i.e. $f \geq 4TeV$, the mixing angles are less restricted and they are in the range $0.15 \leq s \leq 0.99$ and $0.4 \leq s' \leq 0.9$ [10].

Table 1. The vector and axial vector couplings of e^+e^- with vector bosons. Feynman rules for $e^+e^-V_i$ vertices are given as $i\gamma_\mu(g_{V_i} + g_{A_i}\gamma_5)$.

i	vertices	g_{V_i}	g_{A_i}
1	$e^+e^-Z_L$	$\frac{-g}{2c_\text{w}} \left\{ -\frac{1}{2} + 2s_\text{w}^2 - \frac{v^2}{f^2} \left[\frac{-cc_\text{w} x_Z^{W'}}{2s} + \frac{s_\text{w} x_Z^{B'}}{s'c'} \left(2y_e - \frac{9}{5} + \frac{3}{2}c'^2 \right) \right] \right\}$	$\frac{-g}{2c_\text{w}} \left\{ \frac{1}{2} - \frac{v^2}{f^2} \left[\frac{cc_\text{w} x_Z^{W'}}{2s} + \frac{s_\text{w} x_Z^{B'}}{s'c'} \left(-\frac{1}{5} + \frac{1}{2}c'^2 \right) \right] \right\}$
2	$e^+e^-Z_H$	$-gc/4s$	$gc/4s$
3	$e^+e^-A_H$	$\frac{g'}{2s'c'} \left(2y_e - \frac{9}{5} + \frac{3}{2}c'^2 \right)$	$\frac{g'}{2s'c'} \left(-\frac{1}{5} + \frac{1}{2}c'^2 \right)$
4	$e^+e^-A_L$	$-e$	0

In the model, the couplings of vector bosons to fermions are written as $i\gamma_\mu(g_{V_i} + g_{A_i}\gamma_5)$ where $i = 1, 2, 3, 4$ corresponds to Z_L, Z_H, A_H and A_L respectively. The couplings of gauge vector to e^+e^- pairs are given in table 1, where $y_e = \frac{3}{5}$, $e = \sqrt{4\pi\alpha}$, $x_Z^{W'} = -\frac{1}{2c_\text{w}} sc(c^2 - s^2)$ and $x_Z^{B'} = -\frac{5}{2s_\text{w}} s'c'(c'^2 - s'^2)$. The total decay widths of SM vector bosons also get corrections of the order $\frac{v^2}{f^2}$, since the decay widths of vectors to fermion couples are written as; $\Gamma(V_i \to f\bar{f}) = \frac{N}{24\pi}(g_V^2 + g_A^2) M_{V_i}$ where $N = 3$ for quarks, and $N = 1$ for leptons. The total decay widths of the new vector bosons are given as [18]:

$$\begin{aligned}\Gamma_{A_H} &\approx \frac{g'^2 M_{A_H}(21-70s'^2+59s'^4)}{48\pi s'^2(1-s'^2)},\\ \Gamma_{Z_H} &\approx \frac{g^2(193-388s^2+196s^4)}{768\pi s^2(1-s^2)}M_{Z_H}.\end{aligned} \tag{7}$$

The final decays and also the decay widths of ϕ^0 and ϕ^P are studied in detail in Ref.[21], and they are strongly dependent on the VEV of the scalar triplet; v'. For $v' \gtrsim 1GeV$, the decay modes of ϕ^0 include decays in to quark pairs; $t\bar{t}$, $b\bar{b}$ and $t\bar{T}+T\bar{t}$, and also decays into SM pairs; $Z_L Z_L$ and HH. In this case the decays of ϕ^P are similar to ϕ^0 as the decays in to quark pairs; $t\bar{t}$, $b\bar{b}$ and $t\bar{T}+T\bar{t}$, and to SM $Z_L H$ couples different from ϕ^0. For $v' \sim 10^{-10}GeV$, the non leptonic decays are suppressed by a factor of $\frac{v'}{v}$ for both ϕ^0 and ϕ^P, and the final states contain only lepton flavor violating decays to $\nu_i\nu_j + \bar{\nu}_i\bar{\nu}_j$. In this work, we analyze the cases $v' \sim 1GeV \;\; (Y << 1)$ and $v' = 10^{-10}GeV \;\; (Y \sim 1)$. The decay widths of scalars in these cases can be written as[21]:

$$\begin{aligned}\Gamma_{\phi(v'\sim 1)} &\simeq \frac{N_c M_\phi}{32\pi f^2}(M_b^2+M_t^2)+\frac{v'^2 M_\phi^3}{2\pi v^4},\\ \Gamma_{\phi(v'\sim 10^{-10})} &\simeq \Gamma_{\phi(LFV)} = \frac{|Y|^2}{8\pi}M_\phi.\end{aligned} \tag{8}$$

The properties of new neutral scalar ϕ^0, its couplings to SM and new neutral vector bosons can be examined in single production of ϕ^0 associated with Z_L events. The couplings of ϕ^0 to Z_L and vectors are in the form $ig_{\mu\nu}B_i$, where $i = 1, 2, 3$ corresponds to Z_L, Z_H, A_H respectively and given in table 2, where $s_0 \simeq 2\sqrt{2}\frac{v'}{v}$. The Feynman diagrams contributing this process are given in figure 1.

The pair productions of neutral heavy scalar and pseudo scalar associated with Z_L via $e^+e^- \to Z_L\phi^0\phi^0$, $e^+e^- \to Z_L\phi^P\phi^P$ and $e^+e^- \to Z_L\phi^0\phi^P$ are also examined in this work. The Feynman rules for scalar-vector couplings are given in table 2, the Feynman rules for four point scalar(pseudoscalar)-vector couplings are given in table 3 and the Feynman rules for pseudoscalar-vector-scalar couplings are given in table 4, where $s_P = \frac{2\sqrt{2}v'}{\sqrt{v^2+8v'^2}} \simeq 2\sqrt{2}\frac{v'}{v}$. The Feynman diagrams for the processes $e^+e^- \to Z_L\phi^0\phi^0$, $e^+e^- \to Z_L\phi^P\phi^P$ and $e^+e^- \to Z_L\phi^0\phi^P$ are presented in figures 2, 3 and 4 respectively.

Table 2. The Feynman rules for $\phi^0 V_i V_j$ vertices.

i/j	vertices	$ig_{\mu\nu}B_{ij}$
1/1	$\phi^0 Z_L Z_L$	$-\frac{i}{2}\frac{g^2}{c_{\rm w}^2}(vs_0 - 4\sqrt{2}v')g_{\mu\nu}$
2/2	$\phi^0 Z_H Z_H$	$\frac{i}{2}g^2\left(vs_0 + \frac{(c^2-s^2)^2}{s^2c^2}\sqrt{2}v'\right)g_{\mu\nu}$
1/2	$\phi^0 Z_L Z_H$	$\frac{i}{2}\frac{g^2}{c_{\rm w}}\frac{(c^2-s^2)}{2sc}(vs_0 - 4\sqrt{2}v')g_{\mu\nu}$
2/3	$\phi^0 Z_H A_H$	$\frac{i}{4}gg'\frac{1}{scs'c'}\left((c^2s'^2 + s^2c'^2)vs_0\right.$
1/3	$\phi^0 Z_L A_H$	$\frac{i}{2}\frac{gg'}{c_{\rm w}}\frac{(c'^2-s'^2)}{2s'c'}(vs_0 - 4\sqrt{2}v')g_{\mu\nu}$
3/3	$\phi^0 A_H A_H$	$\frac{i}{2}g'^2\left(vs_0 + \frac{(c'^2-s'^2)^2}{s'^2c'^2}\sqrt{2}v'\right)g_{\mu\nu}$

Table 3. The Feynman rules for four point interaction vertices between scalars and vectors. Their couplings are given in the form $iC_{ij}g_{\mu\nu}$ and $iC_{ij}^P g_{\mu\nu}$ respectively for $\phi^0\phi^0 V_i V_j$ and $\phi^P\phi^P V_i V_j$.

i/j	vertices	$iC_{ij}g_{\mu\nu}$	vertices	$iC_{ij}^P g_{\mu\nu}$
1/1	$\phi^0\phi^0 Z_L Z_L$	$2i\frac{g^2}{c_{\rm w}^2}g_{\mu\nu}$	$\phi^P\phi^P Z_L Z_L$	$2i\frac{g^2}{c_{\rm w}^2}g_{\mu\nu}$
1/2	$\phi^0\phi^0 Z_L Z_H$	$-2i\frac{g^2}{c_{\rm w}}\frac{(c^2-s^2)}{2sc}g_{\mu\nu}$	$\phi^P\phi^P Z_L Z_H$	$-2i\frac{g^2}{c_{\rm w}}\frac{(c^2-s^2)}{2sc}g_{\mu\nu}$
1/3	$\phi^0\phi^0 Z_L A_H$	$-2i\frac{gg'}{c_{\rm w}}\frac{(c'^2-s'^2)}{2s'c'}g_{\mu\nu}$	$\phi^P\phi^P Z_L A_H$	$-2i\frac{gg'}{c_{\rm w}}\frac{(c'^2-s'^2)}{2s'c'}g_{\mu\nu}$

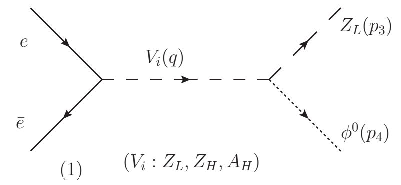

Fig. 1. Feynman diagrams contributing to $e^+e^- \to Z_L\phi^0$ in littlest Higgs model.

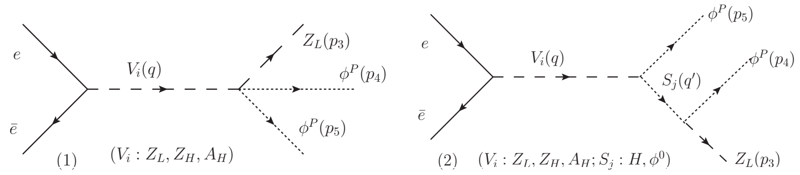

Fig. 2. Feynman diagrams contributing to $e^+e^- \to Z_L\phi^P\phi^P$ in littlest Higgs model.

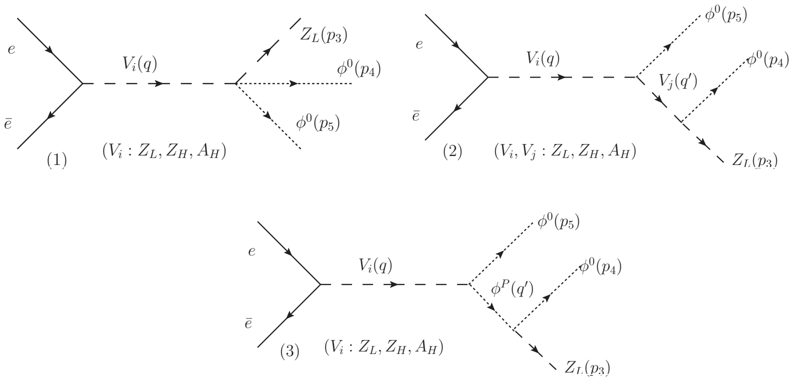

Fig. 3. Feynman diagrams contributing to $e^+e^- \to Z_L\phi^0\phi^0$ in littlest Higgs model.

Table 4. The Feynman rules for $\phi^P V_i S_j$ vertices.

i/j	vertices	$-iE^P_{ij}(p_j - p_{\phi^P})$
1/1	$\phi^P H Z_L$	$\frac{1}{2}\frac{g}{c_{\rm w}}\,(s_P - 2s_0)\,(p_{\phi^P} - p_H)_\mu$
1/2	$\phi^P \phi^0 Z_L$	$-\frac{g}{c_{\rm w}}(p_{\phi^P} - p_{\phi^0})_\mu$
2/1	$\phi^P H Z_H$	$-\frac{1}{2}g\frac{(c^2-s^2)}{2sc}(s_P - 2s_0)(p_{\phi^P} - p_H)_\mu$
2/2	$\phi^P \phi^0 Z_H$	$g\frac{(c^2-s^2)}{2sc}(p_{\phi^P} - p_{\phi^0})_\mu$
3/1	$\phi^P H A_H$	$-\frac{1}{2}g'\frac{(c'^2-s'^2)}{2s'c'}(s_P - 2s_0)(p_{\phi^P} - p_H)_\mu$
3/2	$\phi^P \phi^0 A_H$	$g'\frac{(c'^2-s'^2)}{2s'c'}(p_{\phi^P} - p_{\phi^0})_\mu$

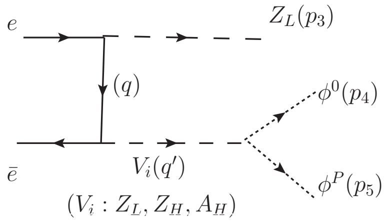

Fig. 4. Feynman diagrams contributing to $e^+e^- \to Z_L\phi^0\phi^P$ in littlest Higgs model.

3. Results and discussions

In this section the results for the processes $e^+e^- \to Z_L\phi^0$, $e^+e^- \to Z_L\phi^0\phi^0$, $e^+e^- \to Z_L\phi^P\phi^P$ and $e^+e^- \to Z_L\phi^0\phi^P$ are presented. The numerical values of the input parameters are taken to be: the Higgs mass $M_H = 120GeV$ and the masses of standard model bosons $M_{Z_L} = 91GeV$, $M_{W_L} = 80GeV$, and the fine structure constant $\alpha = 1/137.036$, consistent with recent data[29]. The numerical calculations of cross sections of the production processes are performed by `CalcHep`[30] generator after implementing necessary vertices.

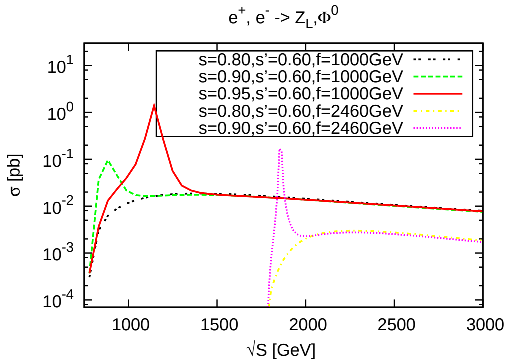

Fig. 5. Total cross section versus center of mass energy graphs of the process $e^+e^- \to Z_L\phi^0$ for some selected values of littlest Higgs model parameters when $v' = 1GeV$.

For the examination of the production of heavy neutral scalar ϕ^0 at linear colliders, the single production of ϕ^0 associated with Z_L is the most dominant channel. For this process, total cross section is plotted with respect to center of mass energy in figure 5 for different values of symmetry breaking scale f and mixing angles s and s' allowed by recent constraints. In these calculations the VEV of the scalar triplet is taken to be $v' = 1GeV$ allowed by the limit given in equation 4. It is seen from figure 5 that, for symmetry breaking scale $f = 1TeV$, and $s/s' = 0.80/0.60$, the total cross section is at the order of $10^{-2}pb$ for $\sqrt{S} \sim 1000 - 3000GeV$. For parameters $f = 1TeV$ and $s/s' = 0.90/0.60(0.95/0.60)$, the total cross section is at the order of $10^{-2}pb$ for $\sqrt{S} \geq 1200(1500)GeV$. Also for these parameter sets, a resonance corresponding to heavy gauge boson Z_H exist at $\sqrt{S} \sim 900(1100)GeV$ increasing the total cross section up to $0.1(1)pb$. Unfortunately these resonances can have significance only if ϕ^0 can be reconstructed. For $f = 2.5TeV$, the cross section versus $\sqrt{S}$ graphs are also plotted in figure 5, for mixing angles $s/s' = 0.80/0.60$ and $s/s' = 0.90/0.60$. In both set of parameters total cross section is about $5 \times 10^{-3}pb$ for $\sqrt{S} \gtrsim 2TeV$. Also for $s/s' = 0.90/0.60$, total cross section receives a peak up to $0.1pb$ about $\sqrt{S} \sim 1.8TeV$ corresponding to the resonance of Z_H. Finally the production of ϕ^0 via $e^+e^- \rightarrow Z_L\phi^0$ process is possible for low values of symmetry breaking scale $f = 1TeV$, for both ILC($\sqrt{S} = 1TeV$) and CLIC($\sqrt{S} = 3TeV$). However for higher values of f, this channel is not promising.

For $v' \sim 1GeV$, the neutral scalar ϕ^0 dominantly decays into quark pairs $t\bar{t}$ and $t\bar{T} + \bar{t}T$, with branching ratios of 0.8 and 0.2 respectively[21]. Thus, the channel $e^+e^- \rightarrow Z_Lt\bar{t}$ is promising for ϕ^0 observation. In this channel, there will be more than thousands events which are observable as a contribution of $e^+e^- \rightarrow Z_L\phi^0$ process. Also in this channel, the SM background is at the order of $10^{-2}pb$ at $\sqrt{S} = 1TeV$, and reduces to $10^{-4}pb$ for $\sqrt{S} \sim 2TeV$. So, for $\sqrt{S} \geq 1TeV$, the collider signal $Z_Lt\bar{t}$ is dominated by the decays of neutral scalars produced via $e^+e^- \rightarrow Z_L\phi^0$ process. And also, by applying a cut on the energy of final state $t\bar{t}$ pair, i.e. $E_{t\bar{t}} \geq M_\phi$, will suppress the background contribution from SM. So in this channel, ϕ^0 can be observed and reconstructed from $t\bar{t}$ jets for $\sqrt{S} \geq 1TeV$.

For the double production of neutral scalar and pseudoscalar via $e^+e^- \rightarrow Z_L\phi^0\phi^0$, $e^+e^- \rightarrow Z_L\phi^P\phi^P$ and $e^+e^- \rightarrow Z_L\phi^0\phi^P$ processes, differential cross section versus energy of Z_L graphs are plotted in figures 6, 7 and 8 respectively, for $f = 1TeV$, and $s/s' = 0.80/0.60, 0.90/0.60, 0.95/0.60$ at $\sqrt{S} = 3TeV$. In these calculations VEV of the scalar triplet is taken to be $v' = 3GeV$. It is seen from the figures that the production rates are not strongly dependent on mixing angles s/s' in the parameter region allowed by electroweak and experimental constraints.

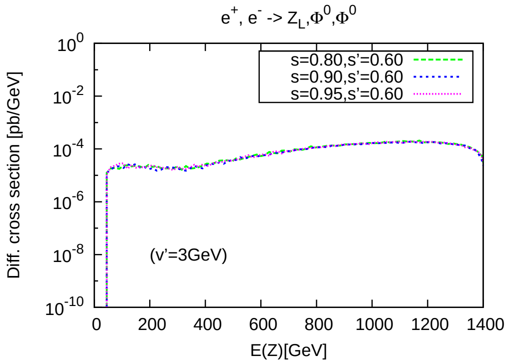

Fig. 6. Differential cross section versus energy of the Z_L boson garphs of the process $e^+e^- \to Z_L\phi^0\phi^0$ for some selected values of mixing angles when $f = 1TeV$ and $v' = 3GeV$ at $\sqrt{S} = 3TeV$.

For the production process $e^+e^- \to Z_L\phi^0\phi^0$, the differential cross section is at the order of $10^{-4}pb/GeV$. The corresponding total cross section is calculated by integrating over E_Z and found to be $0.25pb$. At CLIC, the expected luminosity is $100fb^{-1}$, which will result more than few thousands of production events in this channel. At ILC the expected center of mass energy is about $0.5 - 1TeV$, hence this production channel is out of reach due to kinematical limits from high values of scalar mass M_ϕ.

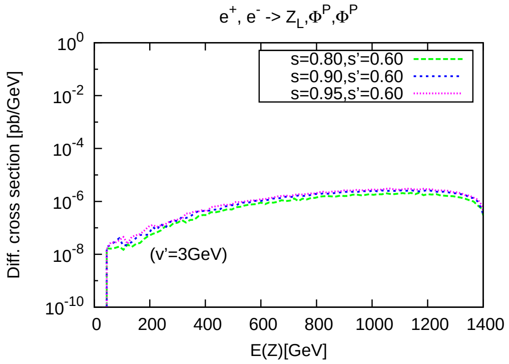

Fig. 7. Differential cross section versus energy of the Z_L boson graphs of the process $e^+e^- \to Z_L\phi^P\phi^P$ for some selected values of mixing angles when $f = 1TeV$ and $v' = 3GeV$ at $\sqrt{S} = 3TeV$.

In the littlest Higgs model, the single production of pseudoscalar ϕ^P associated with Z_L is not allowed. So the most promising channel for ϕ^P production is $e^+e^- \rightarrow Z_L\phi^P\phi^P$. In this channel, the differential cross section is calculated at the order of $10^{-6}pb/GeV$ for all allowed values of mixing angles when $f = 1TeV$(Fig. 7). The maximum value of cross section for this process is calculated as $3 \times 10^{-3}pb$ at $\sqrt{S} = 3TeV$. For an integrated luminosity of $100fb^{-1}$, up to a few hundreds of ϕ^P will be produced within Z_L.

For the process $e^+e^- \rightarrow Z_L\phi^0\phi^P$, the maximum value of differential cross section is about $10^{-8}pb/GeV$. The corresponding total cross section at $\sqrt{S} = 3TeV$ is calculated as $10^{-5}pb$. So in this channel the production rate is not promising.

Table 5. The total cross sections in pb for production of neutral scalars for $f = 1TeV$ and at $\sqrt{s} = 3TeV$ when $v' = 3GeV$ and $v' = 10^{-10}GeV$.

process	$\sigma(pb)[v' = 3GeV]$	$\sigma(pb)[v' = 10^{10}GeV]$
$Z_L\phi^0$	10^{-2}	10^{-23}
$Z_L\phi^0\phi^0$	0.25	2.8×10^{-3}
$Z_L\phi^P\phi^P$	2.8×10^{-3}	2.7×10^{-3}
$Z_L\phi^0\phi^P$	1.0×10^{-5}	1.0×10^{-5}

A distinguishing feature of neutral scalars in littlest Higgs model is their

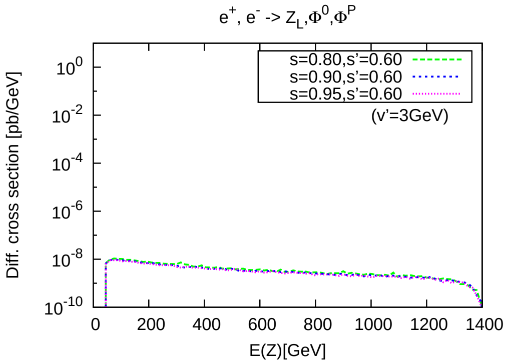

Fig. 8. Differential cross section versus energy of the Z_L boson graphs of the process $e^+e^- \rightarrow Z_L\phi^0\phi^P$ for some selected values of mixing angles when $f = 1TeV$ and $v' = 3GeV$ at $\sqrt{S} = 3TeV$.

lepton flavor violating decay modes. For lepton flavor violation to be dominant, the VEV of the triplet should be at the order $v' = 10^{-10} GeV$. For this value, all other decays of the neutral scalar and pseudoscalar are suppressed. In table 5, the total cross sections of the Z_L associated productions of the neutral scalar and pseudo scalar are given for $s/s' = 0.8/0.6$, $f = 1TeV$ at $\sqrt{S} = 3TeV$ for $v' = 3GeV$ and $v' = 10^{-10} GeV$.

For the process $e^+e^- \to Z_L \phi^0$, at $v' = 10^{-10} GeV$, the production cross section is at the order of $10^{-23} pb$. This is due to the explicit dependence of scalar vector vector couplings on the triplet VEV. Thus, for this channel observation of any lepton flavor violation is not possible.

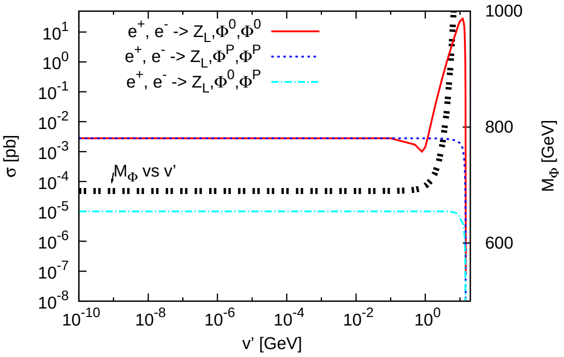

Fig. 9. Thin lines: Dependence of total cross section on the VEV of the scalar triplet v' when $f = 1TeV$ and $s/s' = 0.80/0.60$ at $\sqrt{S} = 3TeV$ for Z_L associated pair production of neutral scalar and pseudoscalar. Thick line: Dependence of heavy scalar mass M_ϕ on v'.

For double production of neutral scalars within Z_L, dependence of cross section on v' is plotted in figure 9, for $f = 1TeV$ at $\sqrt{S} = 3GeV$. It is seen that for $v' < 0.1GeV$, total cross section is not dependent on v'. This is due to mass of the heavy scalars, which is steady with respect to variations of v' in this region(Fig. 9). In figure 10, the total cross sections of the processes $e^+e^- \to Z_L \phi^0 \phi^0$, $e^+e^- \to Z_L \phi^P \phi^P$ and $e^+e^- \to Z_L \phi^P \phi^0$ are plotted with respect to center of mass energy, for $f = 1TeV$, $s/s' = 0.80/0.60$ and $v' = 10^{-10} GeV$. For $v' = 10^{-10}$, the total cross section of the processes $e^+e^- \to Z_L \phi^0 \phi^0$ and $e^+e^- \to Z_L \phi^P \phi^P$ are at the order of $10^{-4} pb$ at $\sqrt{S} \sim 2TeV$, and increases smoothly to $2.8 \times 10^{-3} pb$ as center of mass energy approaches to $3TeV$. Since the value of the Yukawa coupling is $Y \sim 1$ in this scenario, for an integrated luminosity of $100 fb^{-1}$, the number of lepton flavor violating events per year will be close to a thousand. For the process $e^+e^- \to Z_L\phi^P\phi^0$, the total cross section is not sufficient to produce lepton flavor violating events.

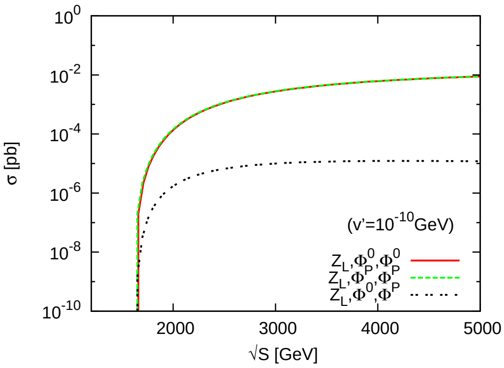

Fig. 10. Dependence of total cross section on center of mass energy when $f = 1TeV$, $v' = 10^{-10}$ and $s/s' = 0.80/0.60$ for Z_L associated pair production of neutral scalar and pseudoscalar.

In figure 11, we have plotted the number of lepton flavor violating final states with respect to v', for a linear collider with an integrated luminosity of $100fb^{-1}$ at $\sqrt{S} = 3TeV$. For these events the collider signature will be *"Z_L+missing energy"*. The SM background in this channel is mostly produced via $e^+e^- \to Z_L\nu\bar{\nu}$ processes which has a total cross section of $5pb$. So for this channel, only applying a constraint on the energy of the Z_L boson can improve the signal background ratio. By choosing Z_L bosons carrying the recoil momentum of the scalar pair, i.e. $E_{Z_L} \geq 2M_\phi$, SM contributions suppressed to 3000 events at $\sqrt{S} \sim 3TeV$. In this case the final state analysis will give important results since this signature makes ϕ^0 and ϕ^P indistinguishable but quite different in appearance from their counter partners in either SM or two Higgs doublet model.

In conclusion, the new heavy scalar ϕ^0 and pseudoscalar ϕ^P of the littlest Higgs model will be produced in e^+e^- colliders associated with Z_L. The production rates significantly depend on the symmetry braking scale parameter f and the vacuum expectation value of the scalar triplet v'. For $f = 1TeV$ and $v' \sim 1GeV$ highest production rates are achieved in both channels. For these parameter set, the productions are quite detectable in the channel $e^+e^- \to Z_L\phi^0$ when $\sqrt{S} > 0.8TeV$ and in the channels $e^+e^- \to Z_L\phi^0\phi^0$ and $e^+e^- \to Z_L\phi^P\phi^P$ when $\sqrt{S} > 1.7TeV$. However in the channel $e^+e^- \to Z_L\phi^0\phi^P$, there is no significant production rate.

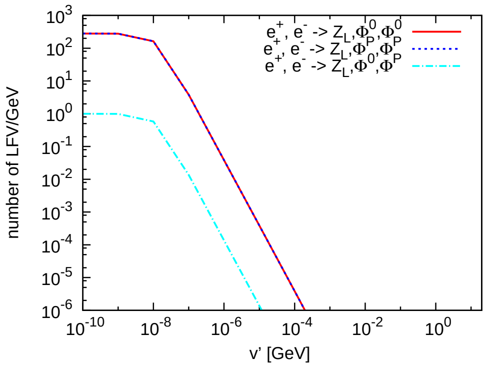

Fig. 11. Dependence of total number of lepton flavour violating final states on the vacuum expectation value of the scalar triplet v' when $f = 1TeV$ and $s/s' = 0.80/0.60$ at $\sqrt{S} = 3TeV$ for Z_L associated pair production of neutral scalar and pseudoscalar.

For higher values of symmetry breaking scale $f \sim 2.5TeV$, the production is achieved only in the channel $e^+e^- \rightarrow Z_L\phi^0$ for $\sqrt{S} \gtrsim 1.8TeV$. For $v' \sim 1GeV$, the channel $e^+e^- \rightarrow Z_L\phi^0$ is the most promising channel for reconstruction of ϕ^0 from $t\bar{t}$ pairs. The effects of the littlest Higgs model heavy scalar can be observed in $Z_Lt\bar{t}$ final states in electron colliders. For $v' \sim 10^{-10}GeV$ and $f = 1TeV$, an interesting and distinguishing feature of the littlest Higgs model is on stage. In this case, final decays of the neutral scalar and pseudoscalar are totally lepton flavor violating with a collider signature of missing energy accompanied by a SM Z_L boson. For this value of v', the productions in the channel $e^+e^- \rightarrow Z_L\phi^0$ is not possible, but in the channels $e^+e^- \rightarrow Z_L\phi^0\phi^0$ and $e^+e^- \rightarrow Z_L\phi^P\phi^P$ the productions of ϕ^0 and ϕ^P are still observable. Although these channels contain high SM background, the productions and final lepton flavor violating decays of ϕ^0 and ϕ^P can still be examined at e^+e^- colliders.

4. Acknowledgments

A. Ç and M.T.Z. thank to T.M Aliev and A. Ç thanks to A. Özpineci, for the guidance and comments.

REFERENCES

[1] N. Arkani-Hamed, A.G. Cohen, E. Katz, and A.E. Nelson, JHEP**0207**(2002)034, `arXiv:hep-ph/0206021`.

[2] N. Arkani-Hamed *et al.*, JHEP**0208**(2002)021, `arXiv:hep-ph/0206020`.T

[3] M. Schmaltz, Nucl.Phys.Proc.Suppl.**117**(2003),`arXiv:hep-ph/0210415`.

[4] D.E.Kaplan and M. Schmaltz, JHEP**0310**(2003)039, `arXiv:hep-ph/0302049`.

[5] J. Hubisz, P. Maeda, A. Noble and M. Perelstein, JHEP**01**(2006)135.

[6] J. L. Hewett, F. J. Petriello and T. G. Rizzo, JHEP **0310** (2003) 062 , `arXiv:hep-ph/0211218`.

[7] M-C. Chen and S. Dawson, Phys.Rev.**D70**(2004)015003, `arXiv:hep-ph/0311032`.

[8] W. Killian and J. Reuter, Phys.Rev. **D70** (2004) 015004, `arXiv:hep-ph/0311095`.

[9] A.G. Dias, C.A. de S. Pires P.S. Rodrigues da Silva, Phys.Rev.**D77**(2008)055001, `arXiv:hep-ph/0711.1154`.

[10] C. Csaki, J. Hubisz, G. D. Kribs, P. Maede and J. Terning, Phys.Rev. **D68** (2003) 035009 , `arXiv:hep-ph/0303236`.

[11] J. A. Conley, J. Hewett and M. P. Le, Phys.Rev.**D72**(2005)115014, `arXiv:hep-ph/0507198v2`.

[12] M. Perelstein, Prog.Part.Nucl.Phys.**58**(2007)247-291, `arXiv:hep-ph/0512128`.

[13] T. Han, H. E. Logan, B. McElrath and L-T. Wang, Phys.Rev. **D67**(2003)095004, `arXiv:hep-ph/0301040`.

[14] M. Schmaltz and D. Tucker-Smith, Ann.Rev.Nucl.Part.Sci.**55**(2005)229-270, `arXiv: hep-ph/0502182`.

[15] G. Azuelos *et al.*, Eur. Phys. J. C. **3952** (2005) 13.

[16] F. Ledroit, AIPConf.Proc.**903**(2007)245-248, `arXiv:hep-ex/0610005`.

[17] W. Kilian, D. Rainwater and J. Reuter, Phys. Rev. **D 74**, 095003 (2006) [Erratum-ibid. D **74**, 099905 (2006)], [arXiv:hep-ph/0609119].

[18] C-X. Yue, W. Yang and F. Zhang, Nucl.Phys. **B716** (2005) 199-214, `arXiv:hep-ph/0409066`.

[19] A. Cagil, M. T. Zeyrek, Phys.Rev. **D80**055021(2009), `arXiv:hep-ph/0908.3581`.

[20] A. Cagil, `arXiv:hep-ph/1010.0102`.

[21] T. Han, H.E. Logan, B. Mukhopadhyaya and R. Srikanth, Phys.Rev. **D72** (2005) 053007 , `arXiv:hep-ph/0505260`.

[22] S.R. Choudhury, N. Gaur and A. Goyal, Phys.Rev. **D72** (2005) 097702 , `arXiv:hep-ph/0508146`.

[23] C-X. Yue and S. Zhao, Eur.Phys.J.**C50**(2007)897-903, `arXiv:hep-ph/0701017`.

[24] S.R. Choudhury *et al.*, Phys.Rev.**D75**(2007)055011, `arXiv:hep-ph/0612327`.

[25] J. Brau (Ed.) *et al*, By ILC Collaboration, *LC Reference Design Report: ILC Global Design Effort and World Wide Study.*, FERMILAB-APC, Aug 2007, `arXiv:acc-ph/0712.1950`.

[26] R.W. Assmann *et al.*, The CLIC Study Team, *A 3 TeV* e^+e^- *linear collider based on CLIC technology*, CERN 2000-008, Geneva, 2000; E. Accomando *et al.*, By CLIC Physics Working Group, *Physics at the CLIC multi-TeV linear collider.*, CERN-2004-005, `arXiv:hep-ph/0412251`; H. Braun *et al.*, By CLIC Study Team, *CLIC 2008 parameters*, CERN-OPEN-2008-021, CLIC-NOTE-764.

[27] G.L. Fogli *et al*, Phys. Rev. D**70**, 113003(2004); M. Tegmark *et al*, SDSS Collabration, Phys. Rev. D**69**, 103501(2004).

[28] E. W. Otten and C. Weinheimer, Reports on Progress in Physics, 71 (2008) 086201, `hep-ex/0909.2104` ; Z-z Xing, `hep-ph/0907.3014` .

[29] K. Nakamura et al. (Particle Data Group), J. Phys. G 37, 075021 (2010).

[30] A. Pukhov *et al.*, CalcHEP/CompHEP Collab., `hep-ph/9908288` ; `hep-ph/0412191`.